



Cite this: *Chem. Sci.*, 2025, **16**, 19370

All publication charges for this article have been paid for by the Royal Society of Chemistry

## Unveiling leaching–oxidizing–landing paths of Pd single-atom catalyzed Suzuki–Miyaura reaction by ambient mass spectrometry

Yiyan Yin,<sup>a</sup> Xiaorong Wang,<sup>a</sup> Xiyang Ge,<sup>a</sup> Xiaotong Shen,<sup>a</sup> Xiaomin Liu,<sup>a</sup> Xiang Li,<sup>ab</sup> Jin Ouyang  <sup>c</sup> and Na Na  <sup>\*a</sup>

The palladium-catalyzed Suzuki–Miyaura cross-coupling (SMCC) reaction is an essential technique for C–C bond formation. It is considered to occur through two distinct pathways involving homogeneous and heterogeneous mechanisms. However, there is still debate about these mechanisms due to the lack of direct structural evidence in both spatial and temporal terms, especially regarding the conversion of active Pd species. In this study, the Pd single-atom catalyst (Pd SAC) SMCC reaction was monitored in real-time using ambient mass spectrometry (AMS) to study the conversions of Pd species both on the catalyst surface and in the liquid phase. This revealed a leaching–oxidizing–landing path as a contributors to the heterogeneous process which involves heterogeneous oxidative addition, Pd leaching along with transmetallation (rather than oxidative addition), and subsequent oxidation–landing back onto the catalyst surface. The leaching–oxidizing–landing mechanism of Pd active sites during the Pd SAC-catalyzed SMCC reaction provides an explanation for the Pd migration on the catalyst surface. A crucial role of molecular oxygen during the SMCC reaction was revealed and attributed to the redeposition of active Pd species through coordination with the catalyst support. Overall, the leaching–oxidizing–landing mechanism of the SMCC reaction has been revealed and it not only provides insights into mechanistic studies and catalyst designs but also expands AMS applications.

Received 18th June 2025  
Accepted 4th September 2025

DOI: 10.1039/d5sc04480d  
[rsc.li/chemical-science](http://rsc.li/chemical-science)

## Introduction

The palladium-catalyzed Suzuki–Miyaura cross-coupling (SMCC) reaction is a notable method for the selective construction of carbon–carbon (C–C) bonds through the reaction between aryl halides and organoboron nucleophiles.<sup>1</sup> The traditional SMCC reaction is facilitated by homogeneous Pd complexes that are coordinated with different ligands, resulting in major disadvantages of toxicity and the high cost of Pd complexes.<sup>2–5</sup> To address these limitations and improve the recovery and reutilization of solid Pd catalysts upon separation, one possible approach could be moving the reaction from homogeneous to heterogeneous systems.<sup>6</sup> Moreover, upon anchoring single metal atoms on different supports, the Pd single-atom catalyst (Pd SAC) might serve as an ideal catalyst by maximizing the metal utilization while minimizing aggregation

and biotoxicity.<sup>7–9</sup> Generally, the SMCC reaction catalyzed by the Pd SAC could simultaneously involve both heterogeneous processes (occurring on the catalyst surface) and homogeneous processes (facilitated by Pd species in solution), which remain under debate due to the lack of direct structural evidence in both the spatial and temporal terms.

Briefly, the main challenge in unveiling the homogeneous/heterogeneous paths of the SMCC reaction could be the examination of detailed changes of active Pd species throughout a series of conversions.<sup>10</sup> The transformation of Pd species may involve leaching from the solid phase, migration, and landing on supports for subsequent catalytic cycles.<sup>11</sup> Due to the lack of sufficient evidence to directly demonstrate structural changes, the natural role of Pd catalytic species is still under debate.<sup>12–14</sup> Several studies have indicated that the soluble Pd species leaching from the solid support are responsible for the homogeneous SMCC reaction,<sup>15–17</sup> whereas others argue that the active sites for the heterogeneous reaction are located on the solid phase.<sup>18–20</sup> Nevertheless, there may exist a complex correlation between these two mechanisms, and both pathways could simultaneously occur during the SMCC reaction. In addition, the unique structural properties of Pd SACs would present additional difficulties in understanding the complex heterogeneous/homogeneous SMCC paths.<sup>21</sup> Although the roles of ligands on Pd have been studied in heterogeneous

<sup>a</sup>Key Laboratory of Radiopharmaceuticals, Ministry of Education, College of Chemistry, Beijing Normal University, Beijing, 100875, China. E-mail: [nana@bnu.edu.cn](mailto:nana@bnu.edu.cn)

<sup>b</sup>State Key Laboratory for Quality Ensurance and Sustainable Use of Dao-di Herbs, National Resource Center for Chinese Materia Medica, China Academy of Chinese Medical Sciences, Beijing, 100700, China

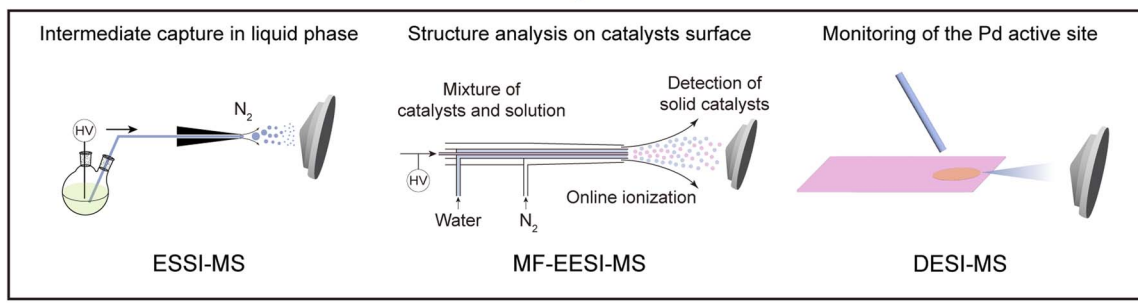
<sup>c</sup>Department of Chemistry, Faculty of Arts and Sciences, Beijing Normal University, Zhuhai, 519085, China



## Pd Single-Atom Catalyzed Suzuki-Miyaura cross-coupling reaction (SMCC reaction)



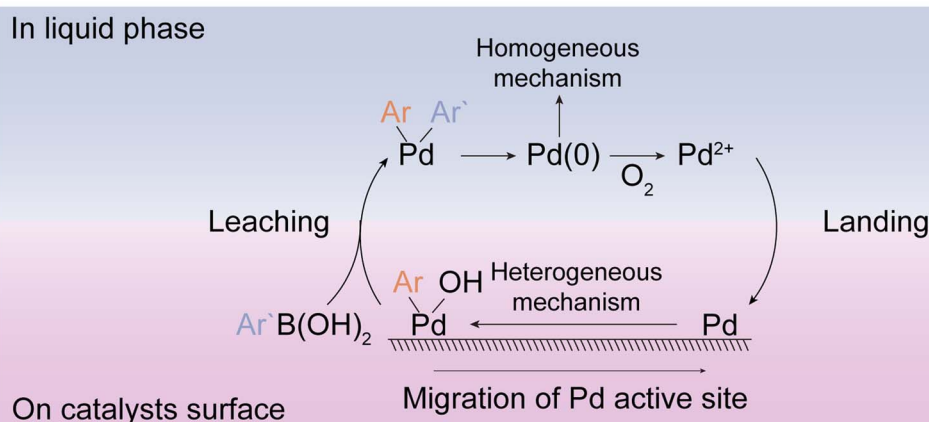
Lack of structural insight during leaching, landing, and migration of Pd active site



Ambient mass spectrometry (AMS) for online monitoring & mechanistic study

- Capture and monitoring of key intermediate
- Structure insights simultaneously on catalysts surface and in liquid phase

## Leaching-Oxidizing-Landing Paths of Pd Single-Atom Catalyzed Suzuki-Miyaura Reaction



**Scheme 1** Ambient mass spectrometry methods for the online monitoring and mechanistic study of the Pd SAC-catalyzed Suzuki–Miyaura cross-coupling reaction.

pathways,<sup>8,22</sup> the detailed Pd transformation during leaching, migration, and the recovery of Pd remains poorly understood. Furthermore, the environmental factors (such as oxygen) affecting the conversion of Pd active sites have not been adequately examined due to the challenge of directly identifying Pd species in real time. Hence, further efforts are necessary to provide structural information on Pd active sites during the leaching and migration of Pd active sites in homogeneous/heterogeneous SMCC paths.

Several strategies have been employed to distinguish, monitor, and examine homogeneous or heterogeneous SMCC paths in spatial and temporal terms, particularly through transmission electron microscopy, real-time fluorescence imaging, and sequential electrical signals.<sup>10,19,23</sup> However, the indirect structural information is still insufficient to clearly identify the structural changes of Pd species during homogeneous/heterogeneous pathways. Ambient mass spectrometry

(AMS) is a label-free technique that allows rapid and direct acquisition of structural information and has shown significant potential for the monitoring of multiple molecules in complex systems.<sup>24–26</sup> With the advantages of online analysis, AMS facilitates the observation and identification of transient intermediates, thereby revealing the roles and changes of active sites.<sup>27–29</sup> Therefore, AMS-based online monitoring would substantially provide multiple pieces of structural information both on the SAC surface and in the liquid phase, facilitating the examination of both leaching and migration of Pd active sites.<sup>30</sup>

In this study, the Pd SAC-catalyzed Suzuki–Miyaura reaction was monitored by a series of AMS methods to investigate fundamental homogeneous/heterogeneous aspects. The AMS monitoring (Scheme 1) was carried out during the SMCC reaction. Structural information regarding both the catalyst surface and the liquid phase illustrates the leaching–oxidizing–landing process of the Pd active site. This study not only offers deeper



insight into the Pd SAC-catalyzed SMCC reaction but also provides an effective AMS method to monitor the structural change of single-atom active sites during the reaction.

## Experimental procedure

### Chemicals

2-Bromopyridine, phenylboronic acid, 2-phenylpyridine, and phosphotungstic acid were obtained from Macklin reagent (Shanghai, China). KOH of analytical grade was purchased from Beijing Chemicals (Beijing, China). Palladium acetate was purchased from Aladdin (Shanghai, China). All other chemical reagents were of analytical grade and were used directly without further purification. Methanol of HPLC grade was purchased from Fisher Chemical (CA, USA). Ultrapure water (Mill-Q, Millipore, 18.2 MΩ) was used in all experiments.

### Instruments

Fourier transform infrared (FTIR) spectra were obtained on a Thermo Scientific Nicolet NEXUS 670. Ultraviolet-visible spectroscopy (UV-vis) measurements were recorded on a Shimadzu UV-3600 spectrophotometer. The yield of the SMCC reaction was analyzed using an Agilent 1260 liquid chromatograph with a mobile phase (acetonitrile/water v/v 6 : 4). HRMS experiments for the liquid phase were performed on a G2-XS QTof mass spectrometer (waters). AMS experiments were performed on an LTQ XL linear ion trap mass spectrometer (Thermo Fisher Scientific).

### Pd@PWO preparation

The Pd@PWO catalyst was prepared following the reported procedures.<sup>31</sup> First, phosphotungstic acid (20.7 g, 6.29 mmol) and KCl (1.00 g, 13.4 mmol) were dissolved in 100 mL water under vigorous stirring. The solution was then adjusted to pH 5.5 by adding KHCO<sub>3</sub> (1 M). After removing the insoluble precipitate, the solution was dried to obtain lacunary PWO. Subsequently, PWO (50 mg, 0.02 mmol) and Pd(Ac)<sub>2</sub> (22.4 mg, 0.10 mmol) were added in 50 mL water. After reacting for 10 h, excess Pd(Ac)<sub>2</sub> was removed by filtering, and the solution was dried and washed with methanol to obtain Pd@PWO.

### SMCC reaction

For the SMCC reaction, 1 mg of Pd@PWO, 1.58 mg of 2-bromopyridine (1 mM), 1.83 mg of phenylboronic acid (1.5 mM), and 1.68 mg of KOH (3 equiv.) were added in 10 mL of methanol. The reaction mixture was stirred at room temperature for 2 h. The solid catalyst was separated by filtration, and the reaction mixture was analyzed by LC.

### Online monitoring of the reaction

An electrosonic spray ionization (ESSI) source was constructed for the online monitoring of the SMCC reaction. A self-pumping effect from the reaction system (i.d. 250 μm; o.d. 365 μm) was generated by a nitrogen stream through an external capillary (i.d. 1000 μm; o.d. 1300 μm). The SMCC reaction mixture was

introduced into the MS inlet and the reactant and product were monitored by MS analysis. MS detection was performed in full scan positive mode over an *m/z* range from 100 to 500. The capillary temperature was 275 °C, and the capillary voltage and tube lens voltage were set at 23.0 V and 75.0 V, respectively. The maximum ion injection time of the linear ion trap was 10 ms. MS results were obtained and analyzed using Xcalibur software.

### Online analysis of the solid catalyst

For the analysis of solid Pd@PWO during the SMCC reaction, a multiphase flow extractive electrospray ionization system (MF-ESSI) was constructed for MS detection. Different from the MF-ESSI system for monitoring the reaction, an interlayer capillary (i.d. 530 μm; o.d. 690 μm) was added for introducing water, promoting the ionization of water-soluble solid catalysts in the spray. MS detection was performed in negative mode over an *m/z* range from 800 to 1000. The capillary temperature was 275 °C, and the capillary voltage and tube lens voltages were set at -26.00 V and -85.35 V, respectively. The maximum ion injection time of the linear ion trap was 1000 ms. MS results were obtained and analyzed using Xcalibur software.

### DESI-MS analysis

A desorption electrospray ionization system (DESI) was used for the MS detection of the solid samples on glass slides with water as the solvent. MS detection was performed in negative mode over an *m/z* range from 800 to 1000. The capillary temperature was 275 °C, and the capillary voltage and tube lens voltage were set to -26.00 V and -85.35 V, respectively. The maximum ion injection time of the linear ion trap was 1000 ms. MS results were obtained and analyzed using Xcalibur software.

## Results

### The feasibility of the SMCC reaction catalyzed by Pd@PWO

With well-defined active sites and ionic structures, a lacunary polyoxometalate-based SAC was chosen as the support for constructing Pd SACs for the SMCC reaction.<sup>32,33</sup> As shown in Fig. 1A, the SMCC reaction was catalyzed by the PW<sub>11</sub>O<sub>39</sub><sup>7-</sup>-derived Pd SAC (Pd@PWO).

Initially, the construction of Pd@PWO was identified by ESSI-MS during the synthesis. As shown in Fig. 1B, the lacunary polyoxometalates were obtained by adjusting the pH of phosphotungstic acid to 5.5, leading to the prominent ion of Keggin-derived lacunary PWO ([PW<sub>11</sub>O<sub>39</sub> + 4H]<sup>3-</sup> at *m/z* 893.72, calc. 893.76) upon removing a W=O group from PW<sub>12</sub>O<sub>40</sub><sup>3-</sup>. Notably, the anionic carrier of the lacunary polyoxometalates possesses high ionization efficiency and facilitates the capture and identification of instantaneous intermediates using the ESSI system. The final Pd@PWO catalyst was successfully characterized upon the coordination of Pd<sup>2+</sup> with four O atoms in the PWO carrier, exhibiting a main ion peak at *m/z* 928.42 (calc. 928.39). This coordination between Pd<sup>2+</sup> and the Keggin-derived lacunary PWO was also confirmed by the UV-Visible absorption spectrum (Fig. S1). Besides, the Pd-coordinated structure of Pd@PWO was further demonstrated by the peaks

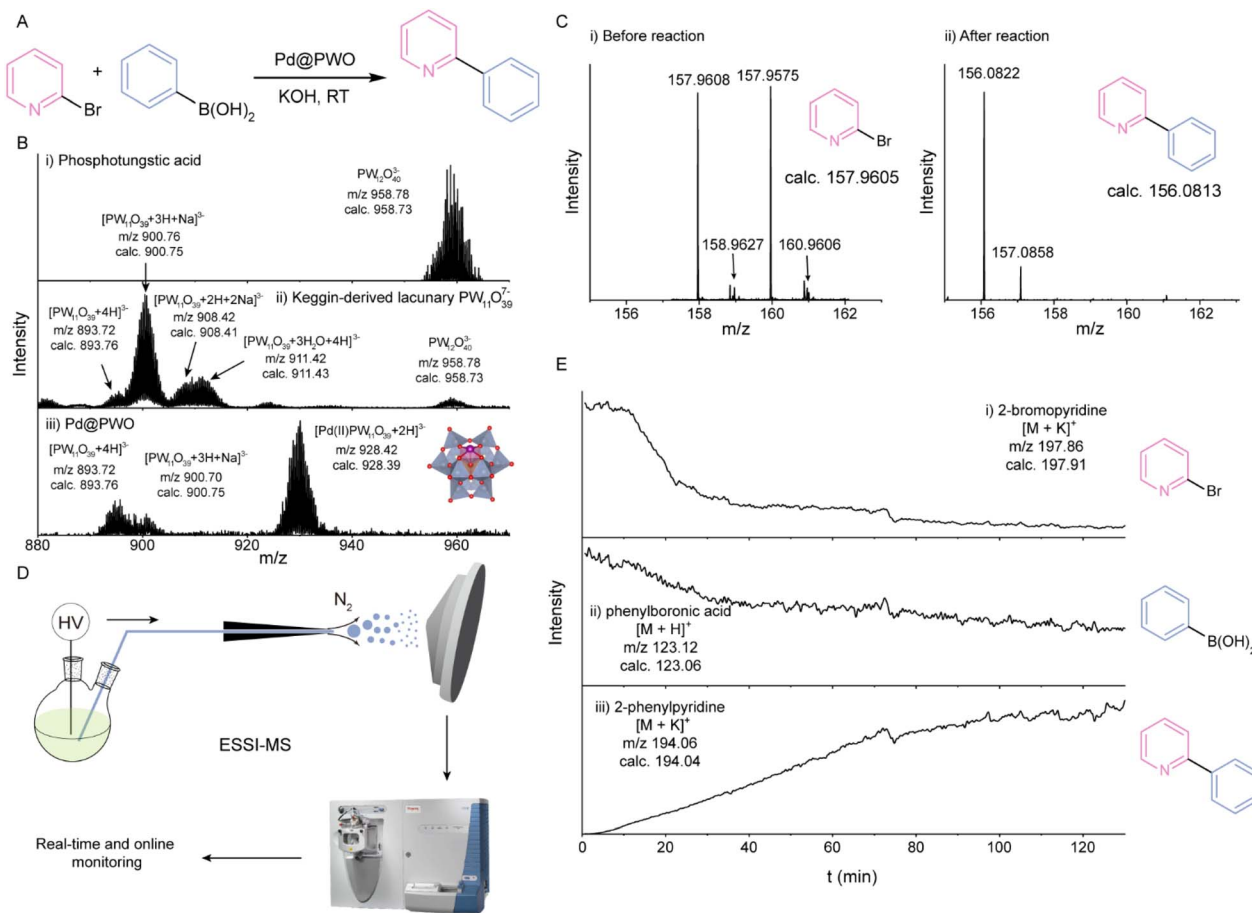


**Fig. 1** Confirmation of Pd@PWO construction and the feasibility of SMCC catalysis. (A) SMCC reaction between 2-bromopyridine and phenylboronic acid to generate the 2-phenylpyridine product was carried out at room temperature (RT) in methanol. (B) Mass spectra of phosphotungstic acid (i), Keggin-derived lacunary PWO (ii), and Pd@PWO (iii). (C) High-resolution mass spectrum of the reaction system before (i) and after the SMCC reaction (ii) for 2 h. (D) Diagram of the ESSI instrument for online monitoring of the SMCC reaction. (E) The extracted ion chromatograms (EICs) of 2-bromopyridine ( $m/z$  197.86) (i), phenylboronic acid ( $m/z$  123.12) (ii), and 2-phenylpyridine ( $m/z$  194.06) (iii) during the SMCC reaction.

(P-Oa at  $\sim$ 1100  $\text{cm}^{-1}$ , W-Ob-W at  $\sim$ 900  $\text{cm}^{-1}$  and W-Oc-W at  $\sim$ 750  $\text{cm}^{-1}$ ) in the infrared absorption spectrum after coordination with Pd (Fig. S2).<sup>34</sup>

Subsequently, the feasibility of the Pd@PWO-catalyzed SMCC reaction between 2-bromopyridine and phenylboronic acid (in the presence of KOH) was examined by liquid chromatography (LC) and HRMS analysis. As demonstrated in Fig. 1C, the reactant 2-bromopyridine ( $[\text{C}_5\text{H}_4\text{NBr} + \text{H}]^+$  at  $m/z$  157.9608, calc. 157.9605) before the reaction and the product 2-phenylpyridine ( $[\text{C}_5\text{H}_4\text{NC}_6\text{H}_5 + \text{H}]^+$  at  $m/z$  156.0822, calc. 156.0813) after the reaction were observed in the HRMS spectra. The relatively high signal intensity of the product indicated an efficient SMCC reaction catalyzed by Pd@PWO, with a 2-phenylpyridine yield of 93% (1 h) at room temperature (determined by LC, Fig. S3). Thereafter, the SMCC reaction was monitored online using ESSI-MS (Fig. 1D). The SMCC reaction system was continuously provided for MS detection through the self-pumping of a nitrogen flow, without any sample pre-treatment or isolation. As shown in Fig. 1E, the decreased reactant

ions of 2-bromopyridine ( $[\text{C}_5\text{H}_4\text{NBr} + \text{K}]^+$  at  $m/z$  197.86, calc. 197.91) and phenylboronic acid ( $[\text{C}_6\text{H}_5\text{B}(\text{OH})_2 + \text{H}]^+$  at  $m/z$  123.12, calc. 123.06), as well as the increased product ions of 2-phenylpyridine ( $[\text{C}_5\text{H}_4\text{NC}_6\text{H}_5 + \text{K}]^+$  at  $m/z$  194.06, calc. 194.04), were observed during the SMCC reaction for 2 h. Furthermore, the product yield was determined to be 97% (determined by LC) in 10 min at a relatively higher temperature of 60 °C (Fig. S4). The turnover number (TON) for the SMCC reaction was 31 and 33 at room temperature and 60 °C, and the turnover frequency (TOF) values were 31 and 198, respectively. ESSI-MS detection demonstrated no SMCC reaction products or additional MS signals at 0 min (Fig. S5A), and the real-time monitoring results of the reaction were basically consistent with LC detection (Fig. S5B). Consequently, any reaction acceleration in the microdroplets generated by ESSI during the SMCC reaction could be excluded. These results demonstrate that Pd@PWO was successfully constructed to efficiently catalyze the SMCC reaction at room temperature, prompting further investigations

to reveal the reaction mechanism in homogeneous and heterogeneous pathways.

### The heterogeneous mechanism of the SMCC reaction under air conditions

To pertinently examine the heterogeneous path or the homogeneous mechanism, the SMCC reaction was monitored for 100 min, with the Pd@PWO being removed at 20 min. Compared to the SMCC reaction catalyzed by Pd@PWO, no significant increase in the yield was recorded after removing Pd@PWO from the system at 20 min (Fig. 2A). This suggests that the heterogeneous mechanism plays a significant role in the SMCC reaction, mostly occurring on the surface of Pd@PWO. Subsequently, to analyze the structural changes of the Pd active sites on the catalyst surface, Pd@PWO during the SMCC reaction was analyzed. For direct and real-time observation of the intermediate structure, multiphase flow extractive electrospray ionization mass spectrometry (MF-EESI-MS)<sup>28</sup> was applied for the online ionization of Pd@PWO during the SMCC reaction. In brief, a MF-EESI system was constructed using 3-layered concentric capillaries. The SMCC reaction system was self-pumping and introduced through the innermost capillary (connected to a high voltage) and electro-sprayed using nitrogen from an external capillary. Simultaneously, a stream of water in the middle layer was introduced (Fig. S6). During MF-EESI, the reaction system within the innermost capillary interacts with

the water spray from the middle layer, facilitating the dissolution of heterogeneous catalysts to accomplish Pd@PWO ionization. As shown in Fig. 2B, in addition to the Pd(II) species of Pd@PWO, an intermediate after the oxidative addition was observed on the surface of the catalyst ( $[\text{Pd(IV)}(\text{C}_5\text{H}_4\text{N})(\text{OH})\text{PW}_{11}\text{O}_{39} + 2\text{H}]^{3-}$  at  $m/z$  960.12, calc. 960.06). Therefore, it can be inferred that the heterogeneous pathway is employed by the Pd(II)-Pd(IV) catalysis. This could be attributed to the strong electron-donating capability of Keggin-derived lacunary PWO, which activates Pd(II) to perform a similar role to that of classical Pd(0) in the SMCC reaction.

Normally, the oxidation of Pd(0) to Pd(II) in the presence of molecular oxygen can decrease the catalytic activity in the traditional Pd-catalyzed SMCC reaction.<sup>35</sup> Predictably, the activation of Pd(II) in Pd@PWO would effectively avoid poisoning of the Pd@PWO catalyst upon molecular oxygen oxidation. Excitingly, the yield of 2-phenylpyridine in air (93%) was significantly higher than that under nitrogen conditions (52%) (Fig. S7). Consequently, molecular oxygen did not reduce the catalytic activity of Pd@PWO but greatly enhanced the efficiency of the SMCC reaction. Meanwhile, a relatively reduced yield (67%) was recorded in oxygen environments, due to the oxidation of phenylboronic acid by the molecular oxygen. Furthermore, this product yield under oxygen conditions (67%) remained higher than that under nitrogen conditions (52%), suggesting that molecular oxygen significantly improves the Pd@PWO-catalyzed SMCC reaction. Although this has also been reported in

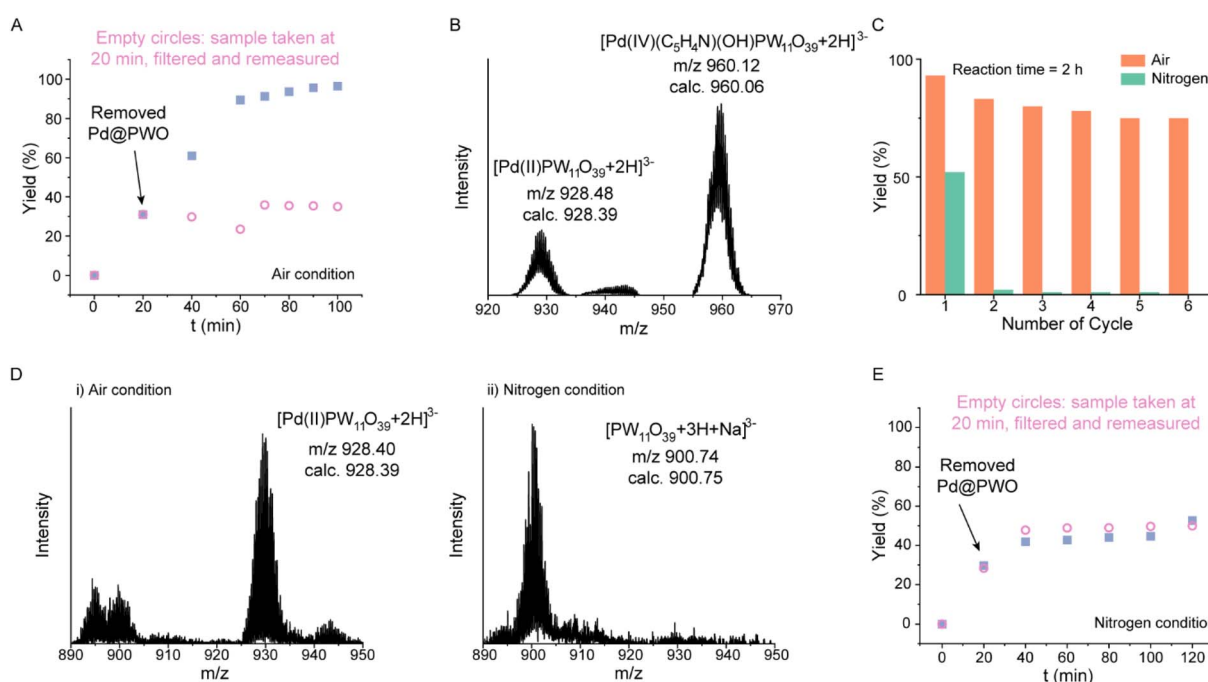


Fig. 2 Examination of the Pd@PWO-catalyzed SMCC reaction under air or nitrogen conditions. (A) Yields of 2-phenylpyridine recorded during 100 min of the SMCC reaction in air. Blue squares: normal monitoring with the time interval injections. Pink circles: monitoring with the catalyst removed at 20 min. (B) Mass spectrum of Pd@PWO isolated from the SMCC reaction at 20 min. (C) Yields of the SMCC reaction catalyzed by the recycled Pd@PWO in several cycles. Six catalytic cycles were employed in both nitrogen and air using the recycled catalyst. The catalysts were washed with methanol and centrifuged after each reaction. (D) Mass spectrum of the isolated Pd@PWO after SMCC reaction under nitrogen conditions (i) and air conditions (ii). (E) Yields of 2-phenylpyridine were recorded during 100 min of the SMCC reaction under nitrogen conditions. Blue squares: normal monitoring with the time interval injections. Pink circles: monitoring with the catalyst removed at 20 min.

some heterogeneous catalysis systems,<sup>19,36</sup> the detailed mechanism of molecular oxygen remains poorly understood. Hence, it is recommended to conduct further investigations into the functions of molecular oxygen, requiring the observation of structural changes of catalysts during the SMCC process.

### The homogeneous mechanism under nitrogen conditions

The influence of molecular oxygen in the SMCC reaction was evaluated by examining the reusability of Pd@PWO in nitrogen and air environments. As shown in Fig. 2C, relatively stable and high yields of the product were obtained across five cycles in air (75–95%). A lower yield was recorded under nitrogen conditions in the first cycle (52%), which declined substantially to less than 5% in the following cycles. The decrease in catalytic activity under nitrogen conditions could be attributed to the structural changes of the Pd@PWO catalyst after the SMCC reaction. To examine the changes in Pd@PWO structures after the SMCC reaction under nitrogen and air conditions, the catalyst was isolated after the reaction for ESSI-MS detection. Under air conditions (Fig. 2D-i), the Pd species of  $[\text{Pd}(\text{II})\text{PW}_{11}\text{O}_{39} + 2\text{H}]^{3-}$  (at 928.40; calc. 928.39) were maintained after the reaction, indicating good reusability of Pd@PWO under air conditions (Fig. 2C). While in nitrogen (Fig. 2D-ii), only the obvious lacunary  $\text{PW}_{11}\text{O}_{39}^{7-}$  ( $[\text{PW}_{11}\text{O}_{39} + 3\text{H} + \text{Na}]^{3-}$  at  $m/z$  900.74, calc. 900.75) was observed after the SMCC reaction. This suggests that Pd active sites were leached from the Pd@PWO catalyst, resulting in poor reusability under nitrogen conditions.

Considering that significant leaching of Pd species would facilitate the SMCC reaction *via* the homogeneous pathway, the SMCC reaction was evaluated by removing Pd@PWO at 20 min under nitrogen conditions. This reaction path was simultaneously compared with the SMCC reaction in nitrogen without catalyst removal. As shown in Fig. 2E, no significant difference was observed between the two reaction systems with or without removing the catalyst at 20 min. This result indicates that the SMCC reaction under nitrogen conditions proceeds through the homogeneous path with leached Pd species in the liquid phase. In general, ligand-free Pd leached into the liquid phase can easily aggregate and lose catalytic activity during the homogeneous SMCC reaction, resulting in the low yield under nitrogen conditions (Fig. S7 and 2C). Therefore, the SMCC reaction under nitrogen follows the homogeneous path, which was dramatically distinct from the heterogeneous reaction in air.

### Examination of the leaching–oxidizing–landing process of Pd species

The leaching of Pd was further investigated due to its critical function in the Pd SAC-catalyzed SMCC reaction. During examination, to ensure satisfactory capture of leaching intermediates, the SMCC reaction was carried out under nitrogen conditions. It is generally believed that the oxidative addition (by 2-bromopyridine) is the prerequisite step for the leaching of Pd.<sup>6</sup> Therefore, the oxidative addition process was initially investigated by evaluating structural changes of Pd@PWO with

the addition of 2-bromopyridine or phenylboronic acid to Pd@PWO. After interacting with the two reactants separately, the catalyst was isolated and analyzed by ESSI-MS to obtain the structural information of Pd@PWO. After interaction with 2-bromopyridine for 2 h, the peak of the Keggin-derived lacunary PWO ( $[\text{PW}_{11}\text{O}_{39} + 3\text{H} + \text{Na}]^{3+}$  at  $m/z$  900.78, calc. 900.75) was recorded, indicating the leaching of the Pd active site from Pd@PWO (Fig. 3A). During interaction between phenylboronic acid and Pd@PWO for 2 h, no obvious signal of lacunary PWO was recorded, indicating the inefficient leaching of Pd species from Pd@PWO. Nevertheless, more efficient leaching of Pd species was observed after the SMCC reaction under nitrogen conditions for only 20 min, with only lacunary PWO observed and no other Pd-related ions recorded (Fig. 3A). Consequently, the oxidative addition process facilitated the leaching of Pd species but was not the main force during the SMCC reaction.

Furthermore, the liquid phase of the SMCC reaction was analyzed using HRMS to investigate the intermediates generated during the leaching of Pd species from Pd@PWO. After 10 min of the reaction, the significant signal peak of  $[\text{Pd}(\text{IV})(\text{C}_5\text{H}_4\text{N})(\text{C}_6\text{H}_5) - \text{H}]^+$  (at  $m/z$  259.9684, calc. 259.9696) was observed in the liquid phase, which was identified as the transmetallation product after leaching from the Pd@PWO catalyst. Furthermore, other potential Pd-related substances (such as oxidative addition species  $\text{Pd}(\text{IV})(\text{C}_5\text{H}_4\text{N})\text{Br}^{2+}$ ) were not detected in the liquid phase. This further demonstrates that the key step of Pd leaching in the SMCC reaction is likely the transmetallation process, rather than the oxidative addition process.

Significantly, a similar transmetallation product  $[\text{Pd}(\text{IV})(\text{C}_5\text{H}_4\text{N})(\text{C}_6\text{H}_5) - \text{H}]^+$  (at  $m/z$  259.9684, calc. 259.9696) was also observed in the SMCC reaction under air conditions (Fig. S8). This suggests that the presence of molecular oxygen did not hinder the leaching of Pd. Therefore, the mechanism of the SMCC reaction under air conditions is not purely heterogeneous, and it involves the leaching of Pd and the efficient recovery of the leached Pd back to the catalyst in the presence of molecular oxygen. Furthermore, the role of molecular oxygen was further demonstrated by observing the recovered Pd on Pd@PWO after a 2 h reaction in nitrogen and another 2 h exposure to air (Fig. S9). Under nitrogen conditions, the leached Pd species was unable to return to the catalyst, leading to homogeneous catalysis in the liquid phase. While under air conditions, the leached Pd species could be oxidized to  $\text{Pd}^{2+}$  by molecular oxygen, which would then be rapidly captured by lacunary PWO to form new Pd active sites through strong interactions. This rapid re-coordination of  $\text{Pd}^{2+}$  to lacunary PWO ensured the excellent reusability of Pd@PWO, sustaining the efficient catalytic activity of the SMCC reaction. Therefore, molecular oxygen was demonstrated to play an important role in the landing of Pd species back to the catalyst and in maintaining the single-atom Pd active sites during the SMCC reaction.

Besides, the intermediate of oxidative addition ( $[\text{Pd}(\text{IV})(\text{C}_5\text{H}_4\text{N})(\text{OH})\text{PW}_{11}\text{O}_{39} + 2\text{H}]^{3-}$ ) was observed on the catalyst during the SMCC reaction under air conditions (Fig. 3B). However, the proposed transmetallation intermediate on the surface of the catalyst of  $[\text{Pd}(\text{IV})(\text{C}_5\text{H}_4\text{N})(\text{C}_6\text{H}_5)\text{PW}_{11}\text{O}_{39} + 2\text{H}]^{3-}$  (calc. 980.08)



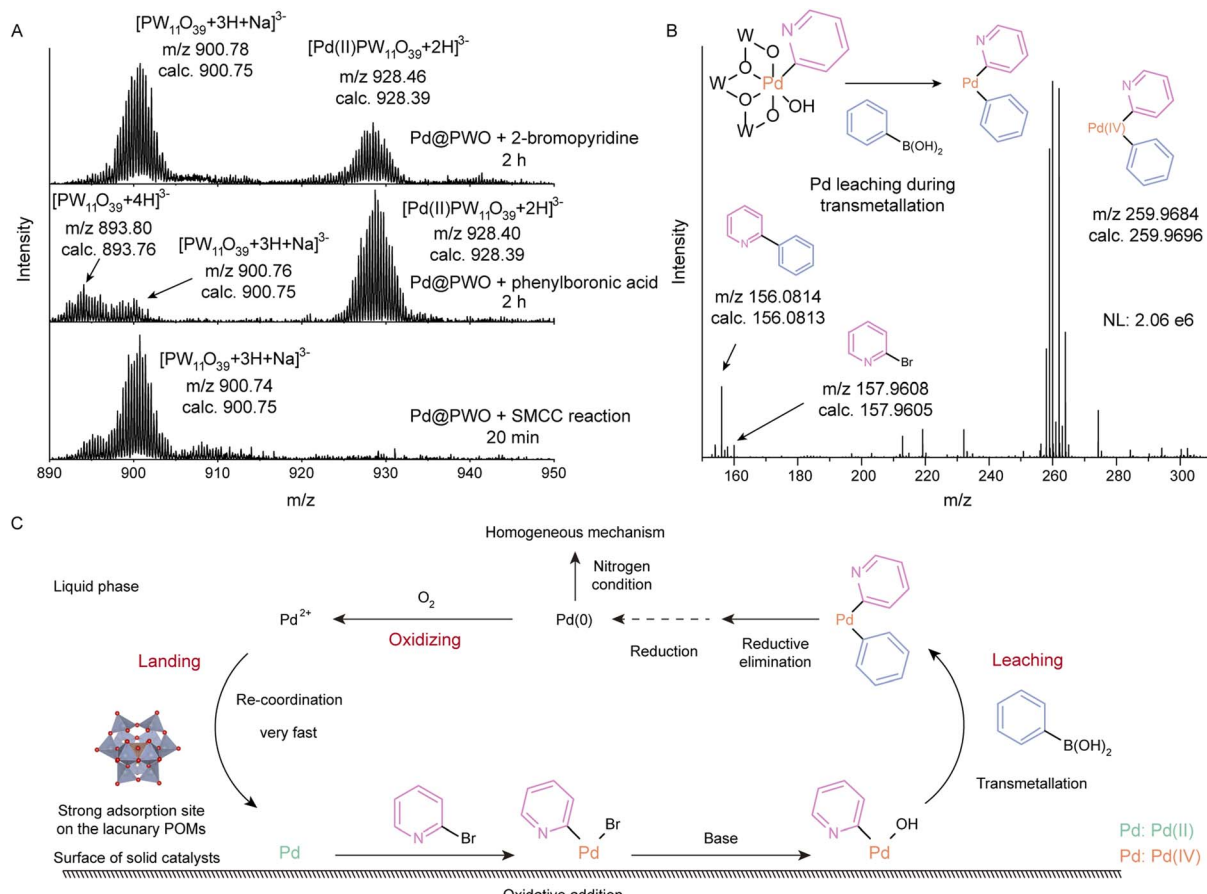


**Fig. 3** Investigation on leaching of Pd species from Pd@PWO. (A) Mass spectra of the isolated Pd@PWO after adding 2-bromopyridine for 2 h, phenylboronic acid for 2 h, and performing the SMCC reaction for 20 min in nitrogen. (B) High-resolution mass spectrum of the liquid phase after SMCC reaction for 10 min in nitrogen. (C) Illustration of the leaching–oxidizing–landing mechanism of the Pd@PWO catalyzed SMCC reaction involving the homogeneous and heterogeneous pathways.

was not observed (Fig. S10). Based on the detection of the intermediate of the transmetallation product in the liquid phase (Fig. S8), it can be further concluded that the leaching of Pd occurs during the transmetallation process rather than the oxidative addition process.

Therefore, based on the monitoring of both catalyst and liquid phase systems, the leaching–oxidizing–landing process of Pd species during the Pd@PWO-catalyzed SMCC reaction was determined. As shown in Fig. 3C, the oxidative addition process occurred on the surface of Pd@PWO. Subsequently, in the presence of phenylboronic acid, the Pd species were leached from the catalyst surface through the transmetallation process. Thereafter, reductive elimination in the liquid phase was carried out, resulting in the generation of leached Pd(0) through reduction by ligands or phenylboronic acid. Due to the difficulty in ionizing neutral leached Pd for MS detection, future research should focus on the mechanism of Pd(0) generation. Under nitrogen conditions, leached Pd(0) undergoes a homogeneous pathway in the liquid phase for the SMCC reaction. In the presence of molecular oxygen, leached Pd is oxidized to  $Pd^{2+}$ , and then quickly coordinates with lacunary PWO to land back on the catalyst surface. This process ensures single-atom Pd

active sites for the subsequent catalytic cycles. In fact, the leaching–oxidizing–landing process not only indicates the role of molecular oxygen in the heterogeneous mechanism but also offers a comprehensive explanation for the migration of Pd active sites.

#### The migration of the active catalytic site of Pd species

The migration of Pd during the SMCC reaction is a significant phenomenon in heterogeneous catalysis, which has been examined by several characterization studies.<sup>10,19</sup> Actually, the proposed landing–oxidizing–landing pathway effectively accounts for the generation of new Pd active sites during the SMCC reaction. Nevertheless, the detailed structural mechanism of migration remains inadequately explained. To confirm the migration of Pd active sites during the SMCC reaction, AMS detection was conducted under air and nitrogen conditions. The direct AMS detection of migration was conducted using a previously reported device with slight modifications.<sup>19</sup> Briefly, a quartz reaction cell with reactants continuously circulated was constructed to magnify the migration tendency (Fig. 4A). To evaluate the migration across a relatively long distance, two catalysts, Pd@PWO and lacunary PWO, were respectively coated

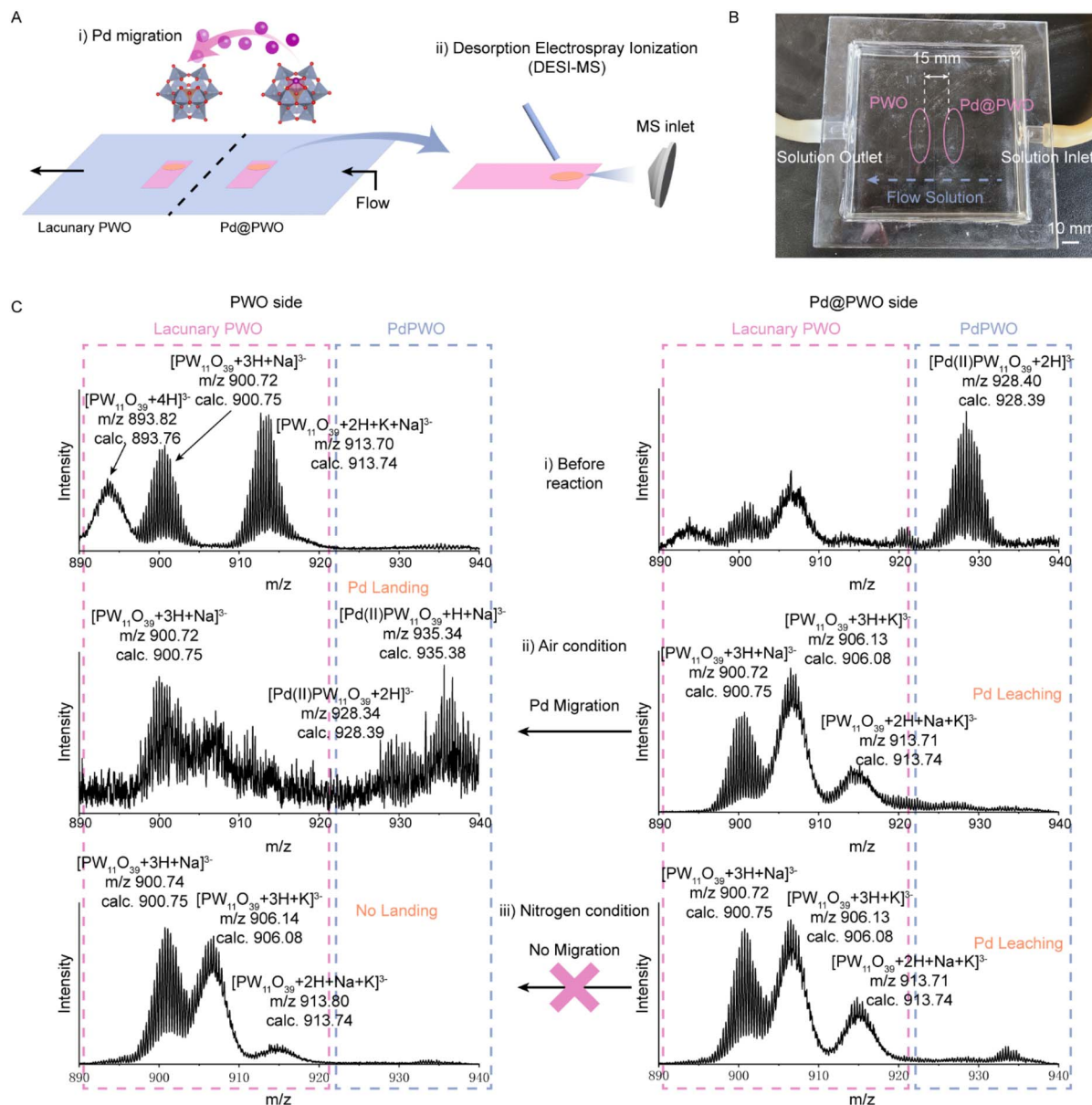


Fig. 4 Evaluation of migration of Pd species from Pd@PWO to lacunary PWO. (A) (i) Schematic illustration of the quartz reaction cell with reactant flow-through. Two glass slides coated with Pd-free lacunary PWO and Pd@PWO catalysts were deposited on the bottom of the cell. (ii) DESI instruments for detecting Pd-related species on two glass slides. (B) Picture of the quartz reaction cell with two sheets located on the cell bottom 15 mm apart. (C) MS spectra of the species on the glass slides with Pd@PWO and PWO before (i) and after the SMCC reaction in air (ii) and nitrogen (iii) for 2 h, respectively. Pink dashed frame: the characteristic peaks of lacunary PWO. Blue dashed frame: the characteristic peaks of Pd@PWO.

on two glass slides and positioned at the cell bottom about 15 mm apart. Subsequently, the reactants 2-bromopyridine and phenylboronic acid were added in methanol and flowed from the Pd@PWO side to the PWO side for the SMCC reaction (Fig. 4B). To verify the proposed migration of Pd active sites during the SMCC reaction, the catalyst on the surface of two glass slides was directly detected by another AMS technique, desorption electrospray ionization mass spectrometry (DESI-MS), without any pretreatment.<sup>25,37</sup> The solvent (water) was electrosprayed onto the glass slides, and the deposited catalysts (Pd@PWO or lacunary PWO) were transported to the mass spectrometer for analysis.

Initially, we assessed the viability of detecting catalysts on the glass slide using DESI-MS. As shown in Fig. 4C, before the SMCC reaction, the main peak of Pd-related species  $[Pd(II) PW_{11}O_{39} + 2H]^{3-}$  (at  $m/z$  928.40, calc. 928.39) was detected on the Pd@PWO-coated side. While on the glass slide with the lacunary PWO coating, only the ions of lacunary PWO ( $[PW_{11}O_{39} + 4H]^{3+}$  at  $m/z$  893.82, calc. 893.76,  $[PW_{11}O_{39} + 3H + Na]^{3-}$  at  $m/z$  900.72, calc. 900.75, and  $[PW_{11}O_{39} + 2H + K + Na]^{3-}$  at  $m/z$  913.70, calc. 913.74) were observed, and no Pd species was identified. This confirms the successful construction of DESI-MS evaluation systems.

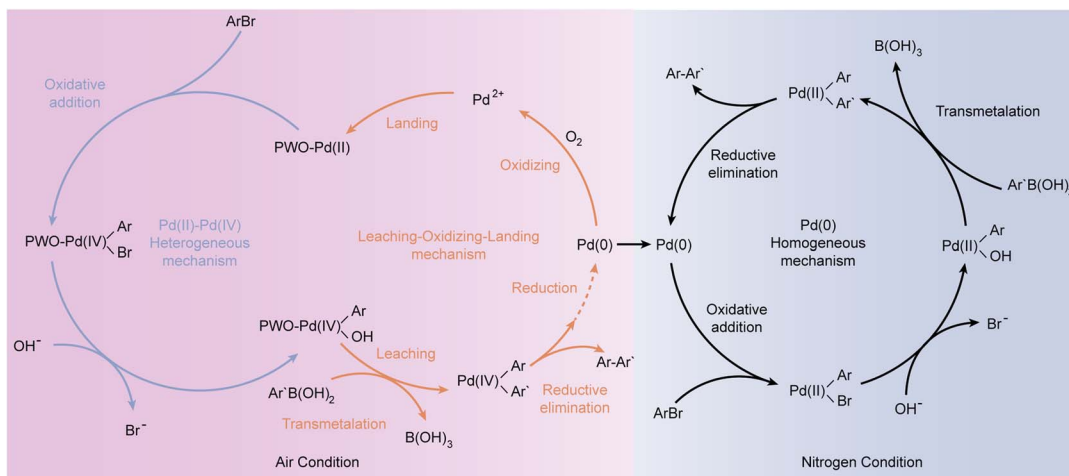


Fig. 5 Catalytic cycles of the Pd(II)-Pd(IV) heterogeneous mechanism (blue), the homogeneous mechanism (black), and the leaching-oxidizing-landing mechanism of Pd species (orange).

To evaluate the oxygen-initiated landing of Pd species during the migration process, the catalytic SMCC reaction was conducted under nitrogen and oxygen conditions for comparison. The reactants flowed from the Pd@PWO side to the PWO side during 2 h of the SMCC reaction in air, and then the two glass slides were detected by DESI-MS. As displayed in Fig. 4C, no significant ion of Pd species was observed on the glass slide originally coated with Pd@PWO, which demonstrated the leaching of Pd active sites, while the corresponding ions of Pd species were detected on the lacunary PWO side ( $[Pd(II)PW_{11}O_{39} + 2H]^{3-}$  at  $m/z$  928.34, calc. 928.39 and  $[Pd(II)PW_{11}O_{39} + H + Na]^{3-}$  at  $m/z$  935.34, calc. 935.38). This experiment validated the migration of Pd active sites, leaching from the Pd@PWO side and subsequently landing on the PWO side. Significantly, the intensity of  $[Pd(II)PW_{11}O_{39} + 2H]^{3-}$  (at  $m/z$  928.42) on the Pd@PWO side dramatically decreased after the SMCC reaction under nitrogen conditions, indicating that the leaching of Pd also occurred in the absence of molecular oxygen. However, no obvious Pd signal was found on the PWO side after the SMCC reaction under nitrogen conditions (Fig. 4C), which indicated no significant landing of Pd species under nitrogen conditions. Consequently, the oxidizing effect of molecular oxygen is crucial for the landing of Pd and further plays a significant role in the migration of Pd active sites. In fact, molecular oxygen facilitates the landing of Pd species back to lacunary PWO upon Pd<sup>2+</sup> coordination, leading to the migration of Pd active sites and thereby maintaining efficient catalytic activity and the reusability of Pd@PWO for the SMCC reaction.

## Discussion

The homogeneous/heterogeneous paths in the SMCC reaction catalyzed by a Pd SAC (Pd@PWO), supported by an anionic ligand (Keggin-derived lacunary  $PW_{11}O_{39}^{7-}$ ), were investigated by AMS monitoring. Although both of the homogeneous and heterogeneous mechanisms have been studied previously,<sup>8,19,23,30</sup> the dynamic changes and conversions of Pd-

species between the catalyst surface and liquid phase remain ambiguous. Upon monitoring by AMS, intermediates on both catalyst surfaces and in the liquid phase were captured and analyzed. This study provides valuable structural information on conversion of Pd-related species between homogeneous and heterogeneous pathways, revealing the leaching-oxidizing-landing process during the SMCC reaction.

Based on identifying intermediates on the catalyst surface and in liquid phases, the leaching of Pd was confirmed under nitrogen conditions. Comparison of leaching between the SMCC reaction and the addition of only the oxidative reactant 2-bromopyridine demonstrates that oxidative addition is not the crucial step in Pd leaching. Oxidative addition products were observed on the catalyst surface, and transmetalation products were observed in the liquid phase rather than on the catalyst surface. Therefore, the transmetalation process may play a crucial role in Pd leaching. Under nitrogen conditions, the leached Pd species follow a homogeneous path in the liquid phase, resulting in poor reusability of Pd@PWO for the SMCC reaction. Nevertheless, due to the technical limitations of the AMS technique, it is not possible to determine the specific mechanism of the reductive elimination process in the liquid phase, since neutral leached Pd is difficult to be ionized for AMS monitoring. Consequently, further studies on the generation of Pd(0) species by reductive elimination are encouraged.

Molecular oxygen does not inhibit the leaching of Pd species in the SMCC reaction under air conditions; rather, it occurs concurrently with the transmetalation process. Furthermore, molecular oxygen facilitates the rapid oxidation and landing of the leached Pd species. In brief, molecular oxygen would further trigger the oxidation of leached Pd(0) to Pd<sup>2+</sup>, facilitating the landing of the Pd active site by coordinating with lacunary PWO. Due to the strong coordination ability of PWO, Pd is able to quickly land back onto the catalyst surface after leaching, resulting in excellent reusability and catalytic activity of Pd@PWO. Given the requirement of anaerobic conditions in the traditional reaction system, understanding this mechanism

will significantly advance the development of the SMCC reaction under air conditions.

This leaching–oxidizing–landing mechanism effectively explains the Pd migration during the SMCC reaction, which was verified by DESI-MS detection. As demonstrated, only the leaching process, but no landing behavior of Pd, was observed under nitrogen conditions. While under air conditions, long-distance migration ( $\sim 15$  mm) of Pd active sites was observed *via* the leaching–oxidizing–landing process. Therefore, molecular oxygen was demonstrated to facilitate the landing of leached Pd species back to the catalyst surface, thereby supporting the leaching–oxidizing–landing mechanism in the SMCC reaction.

## Conclusions

In conclusion, AMS monitoring of the SMCC reaction catalyzed by Pd@PWO suggested the leaching–oxidizing–landing process of Pd, revealing the fundamental aspects of homogeneous/heterogeneous pathways. Heterogeneous oxidative addition between Pd(II) and Pd(IV) was performed on the surface of the Pd@PWO catalyst (Fig. 5). Subsequently, Pd leaching occurred concurrently with the transmetallation process, with reductive elimination occurring in the liquid phase. Under nitrogen conditions, the homogeneous path was employed by the leached Pd species. This process exhibited low catalytic efficiency and poor reusability of Pd@PWO without Pd landing back on the catalyst surface (Fig. 5). This limitation was efficiently overcome in the presence of molecular oxygen. In this way, the subsequent oxidation–landing process was initiated under air conditions (Fig. 5). Significantly, molecular oxygen facilitated the generation of  $\text{Pd}^{2+}$  in the liquid phase, which could efficiently land back onto the catalyst surface. Furthermore, this leaching–oxidizing–landing mechanism effectively explains the migration of Pd active sites on Pd@PWO. The unveiling of leaching–oxidizing–landing paths not only provides new insights into the SMCC mechanism and catalyst designs but also expands the application of AMS in mechanistic investigations.

## Author contributions

Y. Yin, X. Ge, and N. Na conceived the idea and designed the experiments; X. Shen and J. Ouyang supported the characterization of the catalyst; N. Na supervised the project and acquired the funding; Y. Yin, X. Wang, X. Liu and X. Ge conducted the experiments with assistance from N. Na; X. Wang and X. Liu carried out the catalyst synthesis; X. Li carried out the HRMS analysis; Y. Yin, X. Ge, and N. Na analyzed the data and interpreted the results. All authors read, discussed, and commented on the manuscript.

## Conflicts of interest

The authors declare no competing interests.

## Data availability

The data that support the findings of this study are available on request from the corresponding author.

Supplementary information is available. See DOI: <https://doi.org/10.1039/d5sc04480d>.

## Acknowledgements

This study was supported by the National Natural Science Foundation of China (NNSFC, 22274012 and 22474010 to N. N.; 21974010 and 21675014 to J. O.), the National Key Research and Development Program of China (2024YFA1509600 to N. N.) and the Fundamental Research Funds for the Central Universities (No.2233300007 to N. N.).

## Notes and references

- 1 N. Miyaura and A. Suzuki, Palladium-Catalyzed Cross-Coupling Reactions of Organoboron Compounds, *Chem. Rev.*, 1995, **95**, 2457.
- 2 F.-S. Han, Transition-metal-catalyzed Suzuki–Miyaura cross-coupling reactions: a remarkable advance from palladium to nickel catalysts, *Chem. Soc. Rev.*, 2013, **42**, 5270.
- 3 I. Beletskaya P., F. Alonso and V. Tyurin, The Suzuki–Miyaura reaction after the Nobel prize, *Coord. Chem. Rev.*, 2019, **385**, 137.
- 4 S. Handa, Y. Wang, F. Gallou and B. H. Lipshutz, Sustainable Fe–ppm Pd nanoparticle catalysis of Suzuki–Miyaura cross-couplings in water, *Science*, 2015, **349**, 1087.
- 5 C. Torborg and M. Beller, Recent Applications of Palladium-Catalyzed Coupling Reactions in the Pharmaceutical, Agrochemical, and Fine Chemical Industries, *Adv. Synth. Catal.*, 2009, **351**, 3027.
- 6 A. Srivastava, H. Kaur, H. Pahuja, T. M. Rangarajan, R. S. Varma and S. Pasricha, Optimal exploitation of supported heterogenized Pd nanoparticles for C–C cross-coupling reactions, *Coord. Chem. Rev.*, 2024, **507**, 215763.
- 7 Z. Chen, E. Vorobyeva, S. Mitchell, E. Fale, M. A. Ortúñoz, N. López, S. M. Collins, P. A. Midgley, S. Richard, G. Vilé and J. P. Ramírez, A heterogeneous single-atom palladium catalyst surpassing homogeneous systems for Suzuki coupling, *Nat. Nanotechnol.*, 2018, **13**, 702.
- 8 X. Tao, R. Long, D. Wu, Y. Hu, G. Qiu, Z. Qi, B. Li, R. Jiang and Y. Xiong, Anchoring Positively Charged Pd Single Atoms in Ordered Porous Ceria to Boost Catalytic Activity and Stability in Suzuki Coupling Reactions, *Small*, 2020, **16**, 2001782.
- 9 B. Qiao, A. Wang, X. Yang, L. F. Allard, Z. Jiang, Y. Cui, J. Liu, J. Li and T. Zhang, Single-atom catalysis of CO oxidation using Pt1/FeO<sub>x</sub>, *Nat. Chem.*, 2011, **3**, 634.
- 10 A. S. Galushko, D. A. Boiko, E. O. Pentsak, D. B. Eremin and V. P. Ananikov, Time-Resolved Formation and Operation Maps of Pd Catalysts Suggest a Key Role of Single Atom Centers in Cross-Coupling, *J. Am. Chem. Soc.*, 2023, **145**, 9092.



11 D. B. Eremin and V. P. Ananikov, Understanding active species in catalytic transformations: From molecular catalysis to nanoparticles, leaching, "Cocktails" of catalysts and dynamic systems, *Coord. Chem. Rev.*, 2017, **346**, 2.

12 A. V. Gaikwad, A. Holuigue, M. B. Thathagar, J. E. Ten Elshof and G. Rothenberg, Ion- and Atom-Leaching Mechanisms from Palladium Nanoparticles in Cross-Coupling Reactions, *Chem.-Eur. J.*, 2007, **13**, 6908.

13 A. F. Schmidt and A. A. Kurokhtina, Distinguishing between the homogeneous and heterogeneous mechanisms of catalysis in the Mizoroki-Heck and Suzuki-Miyaura reactions: Problems and prospects, *Kinet. Catal.*, 2012, **53**, 714.

14 A. S. Sigeev, A. S. Peregudov, A. V. Cheprakov and I. P. Beletskaya, The Palladium Slow-Release Pre-Catalysts and Nanoparticles in the "Phosphine-Free" Mizoroki-Heck and Suzuki-Miyaura Reactions, *Adv. Synth. Catal.*, 2015, **357**, 417.

15 B. Sun, L. Ning and H. C. Zeng, Confirmation of Suzuki-Miyaura Cross-Coupling Reaction Mechanism through Synthetic Architecture of Nanocatalysts, *J. Am. Chem. Soc.*, 2020, **142**, 13823.

16 B. Li and H. C. Zeng, Minimalization of Metallic Pd Formation in Suzuki Reaction with a Solid-State Organometallic Catalyst, *ACS Appl. Mater.*, 2020, **12**, 33827.

17 W. Shi, Y. Niu, S. Li, L. Zhang, Y. Zhang, G. A. Botton, Y. Wan and B. Zhang, Revealing the Structure Evolution of Heterogeneous Pd Catalyst in Suzuki Reaction *via* the Identical Location Transmission Electron Microscopy, *ACS Nano*, 2021, **15**, 8621.

18 P. J. Ellis, I. J. S. Fairlamb, S. F. J. Hackett, K. Wilson and A. F. Lee, Evidence for the Surface-Catalyzed Suzuki-Miyaura Reaction over Palladium Nanoparticles: An Operando XAS Study, *Angew. Chem., Int. Ed.*, 2010, **49**, 1820.

19 P. Costa, D. Sandrin and J. C. Scaiano, Real-time fluorescence imaging of a heterogeneously catalysed Suzuki-Miyaura reaction, *Nat. Catal.*, 2020, **3**, 427.

20 X. Cai, Y. Liu, G. Li, W. Hu, X. Liu, M. Chen, W. Ding and Y. Zhu, A Functionalized Heterogeneous Catalyst from Atomically Precise Pd<sub>1</sub>Au<sub>8</sub> Clusters Facilitates Carbon-Carbon Bond Construction, *Adv. Mater.*, 2023, **35**, 2301466.

21 R. Lang, X. Du, Y. Huang, X. Jiang, Q. Zhang, Y. Guo, K. Liu, B. Qiao, A. Wang and T. Zhang, Single-Atom Catalysts Based on the Metal-Oxide Interaction, *Chem. Rev.*, 2020, **120**, 11986.

22 M. E. Usteri, G. Giannakakis, A. Bugaev, J. Pérez-Ramírez and S. Mitchell, Understanding and Controlling Reactivity Patterns of Pd<sub>1</sub>@C<sub>3</sub>N<sub>4</sub>-Catalyzed Suzuki-Miyaura Couplings, *ACS Catal.*, 2024, **14**, 12635.

23 C. Yang, L. Zhang, C. Lu, S. Zhou, X. Li, Y. Li, Y. Yang, Y. Li, Z. Liu, J. Yang, K. N. Houk, F. Mo and X. Guo, Unveiling the full reaction path of the Suzuki-Miyaura cross-coupling in a single-molecule junction, *Nat. Nanotechnol.*, 2021, **16**, 1214.

24 X. Zhang, R. Su, J. Li, L. Huang, W. Yang, K. Chingin, R. Balabin, J. Wang, X. Zhang, W. Zhu, K. Huang, S. Feng and H. Chen, Efficient catalyst-free N<sub>2</sub> fixation by water radical cations under ambient conditions, *Nat. Commun.*, 2024, **15**, 1535.

25 Z. Takáts, J. M. Wiseman, B. Gologan and R. G. Cooks, Mass Spectrometry Sampling Under Ambient Conditions with Desorption Electrospray Ionization, *Science*, 2004, **306**, 471.

26 J. Sun, Y. Yin, W. Li, J. Ouyang and N. Na, Chemical Reaction Monitoring By Ambient Mass Spectrometry, *Mass Spectrom. Rev.*, 2022, **41**, 70.

27 X. Liu, J. Chen, Z. Wei, H. Yi and A. Lei, Deciphering reactive intermediates in electrooxidative coupling of indoles through real-time mass spectrometry, *Chem.*, 2024, **10**, 2131.

28 Y. Wang, M. Sun, J. Qiao, J. Ouyang and N. Na, FAD roles in glucose catalytic oxidation studied by multiphase flow of extractive electrospray ionization (MF-EESI) mass spectrometry, *Chem. Sci.*, 2018, **9**, 594.

29 H. Lu, Y. Yin, J. Sun, X. Shen, X. Feng, J. Ouyang and N. Na, Accelerated plasma degradation of organic pollutants in milliseconds and examinations by mass spectrometry, *Chin. Chem. Lett.*, 2021, **32**, 3457.

30 H. Cheng, T. Yang, M. Edwards, S. Tang, S. Xu and X. Yan, Picomole-Scale Transition Metal Electrocatalysis Screening Platform for Discovery of Mild C-C Coupling and C-H Arylation through *in Situ* Anodically Generated Cationic Pd, *J. Am. Chem. Soc.*, 2022, **144**, 1306.

31 Y.-K. Miura and Y. Kamiya, Highly Selective Sorption of Small Polar Molecules by a Nonporous Ionic Crystal of a Lacunary Keggin-type Heteropoly Anion and Alkali Metal Cations, *Chem. Lett.*, 2012, **41**, 331.

32 M. J. Hülsey, G. Sun, P. Sautet and N. Yan, Observing Single-Atom Catalytic Sites During Reactions with Electrospray Ionization Mass Spectrometry, *Angew. Chem., Int. Ed.*, 2021, **60**, 4764.

33 X. Ge, Y. Yin, X. Wang, Y. Gao, X. Guan, J. Sun, J. Ouyang and N. Na, Multienzyme-Like Polyoxometalate-Based Single-Atom Enzymes for Cancer-Specific Therapy Through Acid-Triggered Nontoxicity-to-Toxicity Transition, *Small*, 2024, **20**, 2401073.

34 L. I. Kuznetsova, L. G. Detusheva, M. A. Fedotov and V. A. Likholobov, Catalytic properties of heteropoly complexes containing Fe(III) ions in benzene oxidation by hydrogen peroxide, *J. Mol. Catal. A: Chem.*, 1996, **111**, 81.

35 C. Liu and X. Li, Oxygen-Promoted Suzuki-Miyaura Reaction for Efficient Construction of Biaryls, *Chem. Rec.*, 2016, **16**, 84.

36 C. Liu, C. Liu, X.-M. Li, Z.-M. Gao and Z.-L. Jin, Oxygen-promoted Pd/C-catalyzed Suzuki-Miyaura reaction of potassium aryltrifluoroborates, *Chin. Chem. Lett.*, 2016, **27**, 631.

37 J. Ghosh, J. Mendoza and R. G. Cooks, Accelerated and Concerted Aza-Michael Addition and SuFEx Reaction in Microdroplets in Unitary and High-Throughput Formats, *Angew. Chem., Int. Ed.*, 2022, **61**, e202214090.

